10x GENOMICS

Single Cell and Spatial Technologies to Advance Your Research

Resolve highly complex biological systems, while bringing into focus the details that matter most. Explore biology at true resolution.

Join the conversation with exclusive live talks at Europe-friendly times, or enjoy on-demand recordings at your leisure!

Join the Conversation

Together we succeed!

Get a sneak peek into the progress we're making as a community to optimize single cell and spatial transcriptomics workflows at every step.

10x Genomics & Illumina Coffee-Break Conversations

Learn how single cell sequencing and spatial transcriptomics can unlock biological mysteries across a number of research areas.

10x Genomics European Virtual Scientific Symposium

Learn how single cell and spatial technologies are driving fundamental discoveries across multiple areas of biology, including cancer, immunology, neuroscience—and COVID-19.

And more...

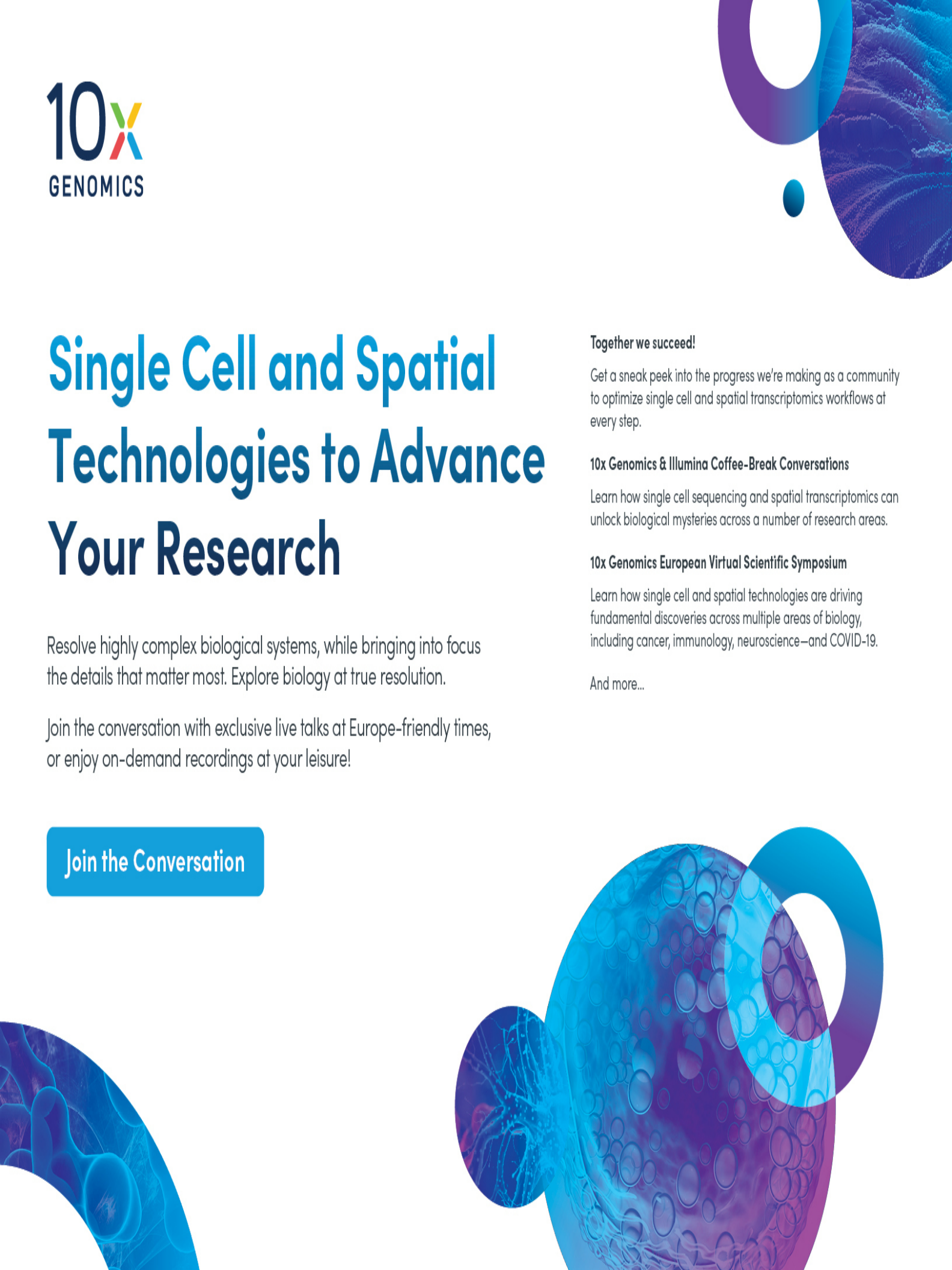

Resolution of inflammation by retrograde chemotaxis of neutrophils in transgenic zebrafish

Jonathan R. Mathias,* Benjamin J. Perrin,* Ting-Xi Liu,[†,1] John Kanki,[†] A. Thomas Look,[†] and Anna Huttenlocher[*,2]

**Department of Pharmacology, University of Wisconsin-Madison, Madison, Wisconsin, USA; and [†]Department of Pediatric Oncology, Dana-Farber Cancer Institute, Boston, Massachusetts, USA*

Abstract: Neutrophil chemotaxis to sites of inflammation is a critical process during normal immune responses to tissue injury and infection and pathological immune responses leading to chronic inflammation. Although progress has been made in understanding the mechanisms that promote neutrophil recruitment to inflamed tissue, the mechanisms that regulate the resolution phase of the inflammatory response have remained relatively elusive. To define the mechanisms that regulate neutrophil-mediated inflammation in vivo, we have developed a novel transgenic zebrafish in which the neutrophils express GFP under control of the myeloperoxidase promoter (zMPO:GFP). Tissue injury induces a robust, inflammatory response, which is characterized by the rapid chemotaxis of neutrophils to the wound site. In vivo time-lapse imaging shows that neutrophils subsequently display directed retrograde chemotaxis back toward the vasculature. These findings implicate retrograde chemotaxis as a novel mechanism that regulates the resolution phase of the inflammatory response. The zMPO:GFP zebrafish provides unique insight into the mechanisms of neutrophil-mediated inflammation and thereby offers opportunities to identify new regulators of the inflammatory response in vivo. *J. Leukoc. Biol.* 80: 1281–1288; 2006.

Key Words: *GFP · leukocyte*

INTRODUCTION

Neutrophil chemotaxis to sites of inflammation is essential during normal immune responses to tissue injury and infection and also contributes to the development of chronic inflammatory diseases such as arthritis and asthma. A better understanding of the mechanisms that regulate leukocyte recruitment and retention in inflamed tissues will provide insight into the pathogenesis of inflammation and will also pave the way for the development of novel therapeutic approaches that dampen or limit the inflammatory response. However, the mechanisms by which inflammation is limited or resolved have remained relatively elusive, to a large extent, as there are few model systems that allow imaging of the inflammatory process in vivo.

The zebrafish, *Danio rerio*, has emerged as a powerful model organism to study disease mechanisms, as it is amenable to genetic and small molecule screens [1–3] and has recently been used to study the development of the immune system [4]. Zebrafish embryos develop several immune cells homologous to mammalian counterparts, including lymphocytes, monocyte/macrophages, and neutrophils [5–7]. Zebrafish neutrophils can be identified by the expression of the neutrophil-specific protein myeloperoxidase (MPO; also referred to as myeloid-specific peroxidase). Zebrafish MPO (zMPO) mRNA expression can be detected as early as 18 h postfertilization (hpf) within the intermediate cell mass (ICM), a posterior region between the notochord and trunk, and by 3 days postfertilization (dpf), zMPO expression can also be seen in circulating blood cells [8, 9]. The presence of several hematopoietic cell types early in development makes zebrafish embryos an ideal model system to analyze leukocyte migration and inflammatory processes in vivo.

There has been substantial recent interest in understanding the resolution phase of the inflammatory response [10, 11]. Recent reviews suggest that the key mechanism by which neutrophil-mediated inflammation is resolved is by the regulated apoptosis of neutrophils in injured tissue [12, 13]. Here, we provide evidence for an alternative mechanism by which neutrophil-mediated inflammation may be resolved by the retrograde migration of neutrophils from injured tissue back to the vasculature. We have generated a novel transgenic zebrafish that expresses GFP in neutrophils under the control of the zMPO promoter. We have used this transgenic fish to visualize neutrophil-mediated inflammation in vivo and have observed bidirectional neutrophil chemotaxis between sites of tissue injury and the vasculature. This transgenic zebrafish will provide a novel genetic model to further dissect the mechanisms involved in the inflammatory response in vivo.

[1] Current address: Shanghai Jiao Tong University School of Medicine, Room 408, Building 1, 225 South Chong Qing Road, Shanghai, China 200025.

[2] Correspondence: Department of Pharmacology, University of Wisconsin-Madison, 2715 Medical Sciences Center, 1300 University Ave., Madison, WI 53706. E-mail: huttenlocher@wisc.edu.

Received May 23, 2006; revised July 3, 2006; accepted August 14, 2006; doi: 10.1189/jlb.0506346.

MATERIALS AND METHODS

Zebrafish maintenance

Adult AB zebrafish (founders purchased originally from the Zebrafish Resource Center, Eugene, OR) and embryos were maintained according to standard protocols [14] and staged as established previously [15]. For wounding assays, zebrafish embryos at 3–4 dpf were anesthetized in E3 containing 0.1 mg/ml Tricaine (ethyl 3-aminobenzoate, Sigma Chemical Co., St. Louis, MO) and then wounded with the tip of a 25-gauge needle. To prevent pigment formation, some embryos (as indicated) were maintained in E3 containing 0.2 mM N-phenylthiourea (PTU; Sigma Chemical Co.).

Endogenous MPO activity assay

Embryos were fixed in 4% paraformaldehyde/PBS for 2 h at room temperature. To detect MPO activity, a Sigma kit (Catalog #390-A) was used as follows: Embryos were washed in1× Trizmal (pH 6.3) containing 0.01% Tween-20 (TT buffer) and then incubated at 37°C in TT containing 1.5 mg/ml substrate (supplied) and 0.015% hydrogen peroxide (from a 30% stock) for 15–30 min. Labeled embryos were then washed in PBS and observed.

Live microscopy of zebrafish embryos

For all movies, embryos were maintained in E3 containing 0.1 mg/ml Tricaine. For **Supplemental Movie 1**, the embryo was embedded in 1% low-melt agarose, and differential interference contrast (DIC) images were captured (30 s/frame for 3 h) using a Nikon Eclipse TE300 inverted microscope, equipped with a 40× DIC objective (NA=0.75), epifluorescent illumination, and a Hamamatsu Orca II charged-coupled device camera. For **Supplemental Movie 2**, images were captured (10 s/frame for 20 min) using a Nikon SMZ-1500 zoom microscope equipped with epifluorescence and a CoolSnap ES camera (Roper Scientific, Duluth, GA). For **Supplemental Movie 3**, DIC and fluorescence images were captured (60 s/frame for 4 h) using the same microscope and equipment as for Supplemental Movie 1, except that a 20× DIC objective (NA=0.45) was used. All images were captured and analyzed with MetaMorph software; shifts in embryo position were corrected by realigning adjacent images using the "Align" tool, and areas of pigmentation served as markers. Movies were converted to audio video interleave format using MetaMorph and compressed using QuickTime Player Version 7.0.4.

Cloning zMPO promoter and construction of zMPO:GFP plasmid

The BUSM1 P1 artificial chromosome clone (PAC) library (RZPD, Germany) was screened for a PAC containing the zMPO genomic sequence using a ^{32}P-labeled probe containing the sequence of the zMPO cDNA (Accession #AF349034). A zMPO-positive library clone containing 120 kb was isolated and digested with *Bgl*II to release a 10-kb fragment, which was subcloned into pBlueScript SK+/− (Stratagene, La Jolla, CA). This subclone was digested with *Xho*I and *Cla*I to release an ~8-kb fragment (see Fig. 2A) of the zMPO 5′-untranslated region. A PCR-generated linker comprising the region from the *Cla*I site to the start of the zMPO open-reading frame (with a *Bam*HI site introduced just upstream) was amplified from the *Bgl*II subclone using the following primers: GTGAGCCTGAGACACGCATG (forward) and GC**GGATC-C**CTCTAAAAACACATATTG (reverse; *Bam*HI site in boldface).

A *Bam*HI/*Xho*I fragment containing GFP and a SV40 polyadenylation sequence (Clontech, Palo Alto, CA) were ligated with the *Cla*I/*Bam*HI-digested PCR linker and the 8-kb *Xho*I/*Cla*I genomic fragment into *Xho*I-digested pBlueScript SK+/−, resulting in the zMPO:GFP construct (see Fig. 2B).

Generation of transgenic zMPO:GFP lines

The zMPO:GFP plasmid was resuspended at 50 pg/nl in Danieau buffer [58 mM NaCl, 0.7 mM KCl, 0.4 mM $MgSO_4$, 0.6 mM $Ca(NO_3)_2$, 5.0 mM HEPES, pH 7.6], and 7.5 pg was injected into the cytoplasm of one-cell stage embryos, which were raised to sexual maturity and crossed to wild-type zebrafish to produce F1 embryos that were screened for cellular GFP expression in the ICM at 2–3 dpf.

Antibody production

The zMPO open-reading frame was PCR-amplified from a zMPO cDNA (Accession #AF349034 in pBK-CMV) using the following primers: AGAAC-TA**GTCGAC**AGTGTTGTGCTCTTTCAGTGG (forward; *Sal*I site in boldface) and ATAAGTAA**GCGGCCGC**AACATCCCTGAGGTTTGGTTATA (reverse; *Not*I site in boldface). This PCR product was digested with *Sal*I and *Not*I and subcloned into *Sal*I/*Not*I-digested pGEX-4T-1 (Amersham, UK) to produce pGST-zMPO, and the GST-zMPO fusion protein expressed from this plasmid was purified and used to raise a rabbit polyclonal antibody as described previously [16].

Whole-mount immunofluorescence

Embryos were fixed for 2 h in 1% formaldehyde (Electron Microscopy Sciences, Hatfield, PA) in PBS and washed in PBS and then PBS containing 0.15 M glycine (Sigma Chemical Co.). Emrbyos were next washed in methanol at –20°C and rehydrated in a graded series of methanol in PBS containing 0.2% Triton X-100 (PBS-TX). Embryos were blocked in PBS-TX containing 1% (w/v) BSA and incubated overnight at 4°C in the rabbit polyclonal antibody to zMPO (described above) diluted in blocking medium. Following several washes in PBS-TX, embryos were incubated for 3–4 h in a tetramethylrhodamine isothiocyanate-conjugated goat anti-rabbit antibody (Jackson ImmunoResearch Laboratories, West Grove, PA) diluted in blocking medium. Embryos were washed in a graded series of glycerol in PBS-TX, the last wash containing 1 mg/ml 1,4-diazabicyclo-[2.2.2]octane (Sigma Chemical Co.) as an anti-photo-bleaching agent. Fluorescence in immunolabeled embryos was observed using a Nikon SMZ-1500 zoom microscope or a Nikon Eclipse TE300 inverted microscope and imaged with MetaMorph software.

To immunolabel transgenic zMPO:GFP embryos, the same protocol was used with the following modifications to preserve GFP fluorescence: Embryos were fixed in 6% paraformaldehyde/PBS for 2 h at room temperature and then overnight at 4°C in 4% paraformaldehyde/PBS. Following fixation, embryos were washed in PBS, then PBS-TX, and then TBS (150 mM NaCl, 15 mM Tris, pH 7.4) containing 0.01% Tween-20 (TBST). To quench background autofluorescence, embryos were treated twice with sodium borohydride (Sigma Chemical Co., 1 mg/ml in TBST) for 15 min with periodic inversion. Methanol washes (and subsequent rehydration) were omitted, as this was observed to remove GFP fluorescence.

Flow cytometry of adult zebrafish hematopoietic cells

Hematopoietic cell isolation (blood and whole kidney marrow) and flow cytometry were performed as described previously [17, 18] using a FacsScan single laser (488 nM argon ion) bench-top cytometer. Note that heparin (American Pharmaceutical Partners, Schaumburg, IL) was added to media (at 10 units/ml) used for live cells. GFP-positive cells were determined according to viability (propidium iodide exclusion), autofluorescence (i.e., lacking red fluorescence), and green fluorescence expression. Flow cytometry data were analyzed using FloJo software (TreeStar, Inc., Ashland, OR). Data (see Fig. 3) were obtained from cells isolated from individual fish on different days and represent results obtained from analysis of cells from at least three individuals.

Cell tracking and cell speed measurement

Individual cells (n=25 neutrophils, n=11 low GFP-expressing cells described in the text) were tracked using the "Track point" function of MetaMorph and average cell speeds calculated as described previously [19]. Each cell was tracked as long as it could be distinguished from other migrating cells. Cell tracks were generated using MS Excel and overlaid onto individual images from movies (see Fig. 6). To calculate velocity and persistence of migration directionality (see Fig. 7), cell centroid positions of zebrafish neutrophils were tracked toward the wound (n=20) and toward the vasculature (n=20) using the Track point function of MetaMorph. Directionality index (D/T) was calculated by determining the shortest linear distance (D) between the start point and end point of the migration path compared with the total distance traveled by the cell (T) as described previously [20]. The higher the D/T (0.7–1.0) indicates highly directional migration and a loss of random motility.

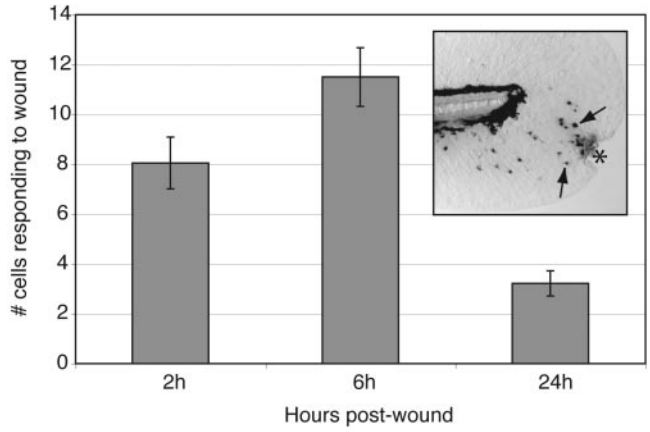

Fig. 1. Quantification of neutrophil recruitment in response to wounding. Zebrafish embryos at 4 dpf were wounded in the tailfin and allowed to recover for the indicated times (*x*-axis). At each time-point, ~25 embryos were fixed and assayed for MPO activity; the inset box shows an example of a tailfin that was wounded (*) and labeled using the MPO activity assay. The number of MPO-positive cells (examples marked with arrows) responding to each wound was counted and averaged (*y*-axis; error bars indicate SEM) for each time-point. Note that there were consistently no MPO-positive cells in the tailfins of embryos fixed immediately after wounding.

RESULTS

Leukocyte recruitment in response to tissue injury in zebrafish embryos

Previous studies have demonstrated that neutrophil-mediated inflammation can be induced in zebrafish embryos by tissue injury. These studies have shown that transection of the tail induces the recruitment of cells that are positive for neutrophil-specific MPO activity and express zMPO mRNA [8]. In accordance with these findings, we performed time-lapse microscopy of zebrafish embryo (3–4 dpf) fins after being wounded (Supplementary Movie 1) and observed the robust recruitment of leukocytes to the site of tissue injury. To quantify this response, wounds were induced in the tailfins of zebrafish embryos (at 4 dpf), and the neutrophil response to wounding was studied in fixed embryos by assaying for MPO activity at different times after wounding. We observed increasing numbers of MPO-positive cells at wound sites up to 6 h postinjury, after which, we consistently observed a decrease in these numbers down to the apparent resolution of the response by 24 h post-injury (**Fig. 1**). To address the mechanism by which this inflammatory response is resolved, we developed a transgenic zebrafish that expresses GFP under the control of the zMPO promoter to enable high-resolution analysis of neutrophil-mediated inflammation in vivo.

Development of a zMPO:GFP transgenic zebrafish

To generate a transgenic zebrafish that expresses GFP in neutrophils, ~8.0 kB of the 5′-untranslated region of the zMPO gene was cloned upstream of GFP (**Fig. 2, A** and **B**). This plasmid construct was microinjected into wild-type zebrafish embryos and shown to transiently express GFP by 22 hpf in distinct cells over the anterior yolk sac and ICM (Fig. 2C). Embryos injected with this construct were raised to ma-

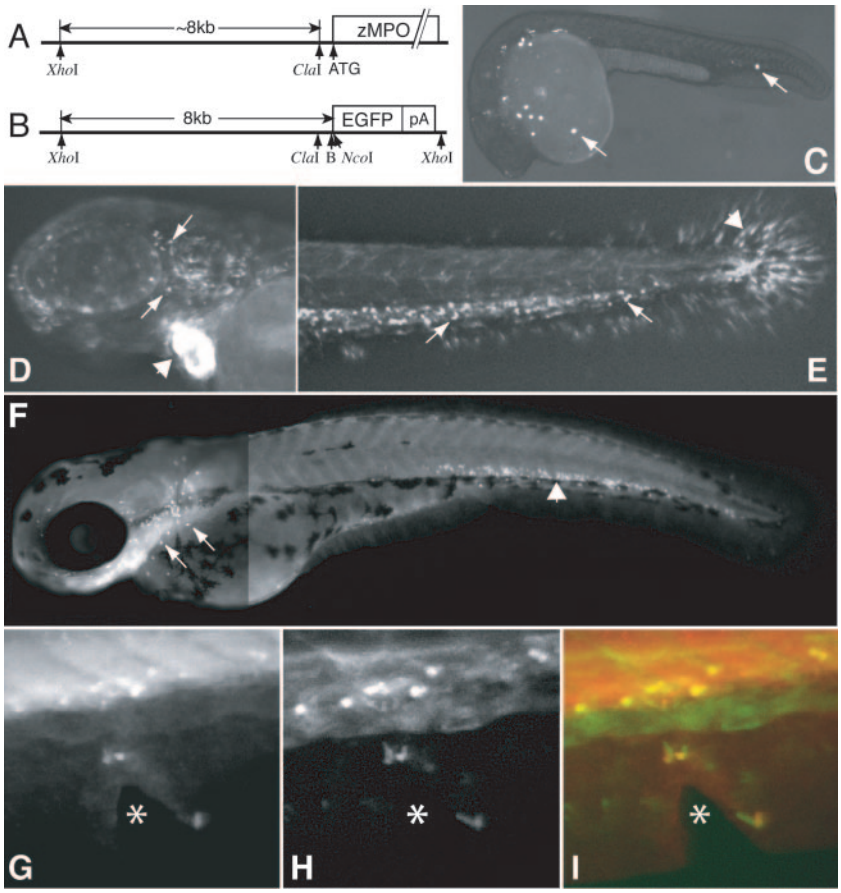

Fig. 2. Generation of zMPO:GFP zebrafish. (A) Restriction map (approximate scale) of the genomic region upstream of the zebrafish MPO open-reading frame. (B) Schematic of the zMPO:GFP construct used to establish transgenic lines by injection into zebrafish embryos. B = *Bam*HI; EGFP, enhanced GFP. (C) Transient expression of the zMPO:GFP construct. Zebrafish embryos were injected with the zMPO:GFP construct at the one-cell stage and allowed to develop in the dark. Shown is a composite fluorescence image of an injected embryo at 22 hpf; anterior is to the left, and dorsal points up. Arrows indicate cells expressing GFP. (D–E) Transgenic zMPO:GFP embryo at 3 dpf; arrows indicate cells expressing GFP. (D) Head region; arrowhead indicates the heart. (E) Tail region; arrowhead indicates GFP expression within tailfin cells. (F) Composite image of wild-type embryo at 3 dpf immunolabeled with a polyclonal antibody (pAb) to zMPO; arrows indicate individual MPO-immunolabeled cells, and arrowhead indicates ICM region. (G–I) zMPO:GFP embryo at 3 dpf after 2 h of response to a wound (*) in the ventral fin. (G) Immunolabeling using the pAb to zMPO. (H) GFP expression. (I) Overlay of G and H, and colocalized areas are yellow.

turity, and three transgenic lines [designated *Tg(zMPO:GFP)*^{uw} and referred to hereafter as zMPO:GFP] were propagated from GFP-positive founders. Expression of the transgene in embryos was observed at several stages (**Supplemental Fig. 1**) and confirmed to exhibit a distribution consistent with zMPO mRNA [8, 9]. It is notable that at 3 dpf, GFP expression was observed in cells around the head and heart (Fig. 2D) and within the ICM (Fig. 2E). To confirm that GFP is expressed in cells that also express zMPO, we developed an antibody to the zMPO protein that labels cells in a similar pattern to zMPO mRNA (Fig. 2F). Cross-reactivity with GFP-expressing cells in zMPO:GFP transgenic embryos was observed in the ICM and at wound sites (Fig. 2, G–I), confirming that the transgenic construct is expressed in cells that also express zMPO. There was also some expression in apparent nonhematopoietic and nonmotile cells (Supplemental Fig. 1; Fig. 2E), which did not label with the zMPO antibody (Fig. 2F) and did not interfere with imaging of zebrafish neutrophils. Together, these findings demonstrate that we have successfully generated a transgenic zebrafish that expresses GFP in embryonic zebrafish neutrophils.

To confirm the neutrophil-specific expression of the zMPO:GFP transgene in adult zebrafish, hematopoietic cells from circulating blood and whole kidney marrow were isolated from transgenic zebrafish and analyzed by flow cytometry. Previous studies have demonstrated that zebrafish hematopoietic cells can be sorted into four groups based on light-scattering characteristics: erythrocyte, lymphocyte/thrombocyte, granulocyte/monocyte, and precursor fractions [17, 18]. Another study has shown that MPO activity can be detected during multiple stages of adult neutrophil development [8], reaching its highest level during precursor stages prior to reaching maturity. Consistent with these results, GFP-positive cells from the principal site of adult blood cell development, whole kidney marrow, were found to cluster predominantly in the precursor and granulocyte/monocyte fractions (**Fig. 3B**). In contrast, GFP-positive cells from circulating blood, where mainly mature blood cells are present, clustered mainly in the granulocyte/monocyte fraction (Fig. 3D). These results confirm further that we have generated a transgenic line which expresses GFP in neutrophils, and we therefore used the transgenic fish to study neutrophil migration in vivo.

In vivo imaging of neutrophil motility in zMPO:GFP transgenic embryos

To observe neutrophil motility in the zMPO:GFP transgenic embryos, live time-lapse fluorescence microscopy of embryos at 3 dpf was performed. In addition to neutrophils circulating through the vasculature, spontaneous neutrophil motility was observed in the head (data not shown), within bodily tissues (**Fig. 4**), and within the ICM (Supplementary Movie 2).

To observe neutrophil chemotaxis in vivo, zMPO:GFP embryos were wounded in the fin at 3 dpf (Supplemental Movie 3). Wounding induced the robust recruitment of neutrophils to the wound site (**Fig. 5**, top) with a range of behaviors and morphologies. During migration, these cells take on a highly polarized morphology, exhibiting a broad, leading edge or pseudopod and a narrow cell rear (**Fig. 6A**). Pseudopod extension and abrupt changes in the direction of migration were frequently observed (Fig. 6C). After migration to the wound site, some neutrophils stop and arrest at the wound, where they develop a rounded morphology and reduced pseudopod extension (Fig. 6B). Other neutrophils continued migration within or around the wound (Fig. 6C). The average speed of migration of zebrafish neutrophils (taken from $n=25$ complete cell tracks)

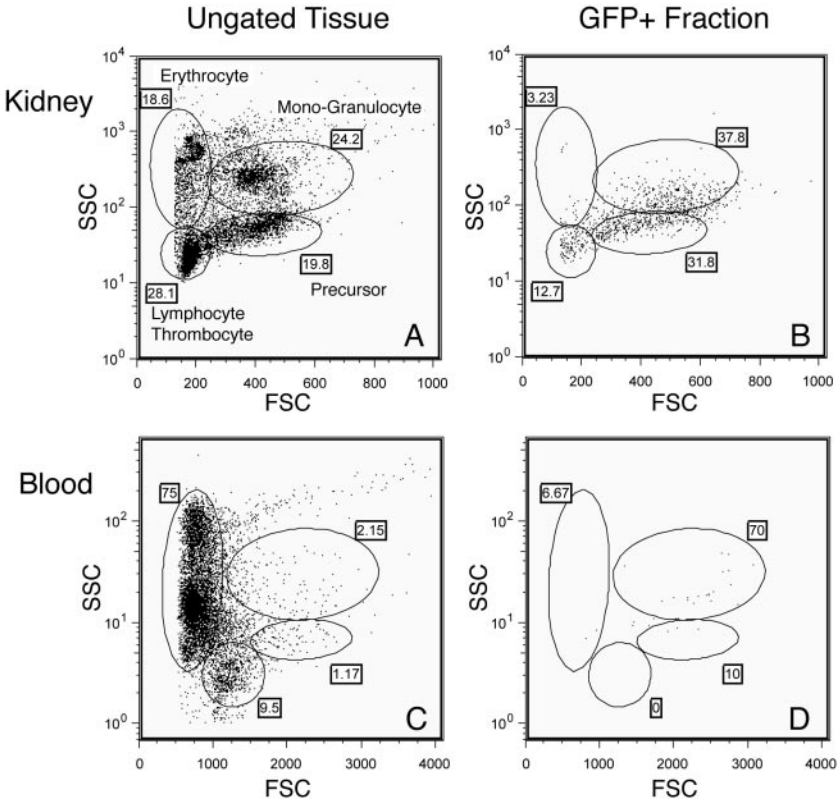

Fig. 3. Flow cytometry of hematopoietic cells from adult transgenic zMPO:GFP zebrafish. Forward-scatter (FSC) and side-scatter (SSC) data were obtained for whole kidney marrow (A) and blood (C) and gates drawn according to cell type based on previous studies [17, 18]. GFP+ cells (determined as detailed in Materials and Methods) from whole kidney marrow (B) and blood (D) were replotted according to FSC and SSC and analyzed using the gates drawn in A and C. For each fraction, the percentage of the total number of cells on the graph is indicated next to each gate.

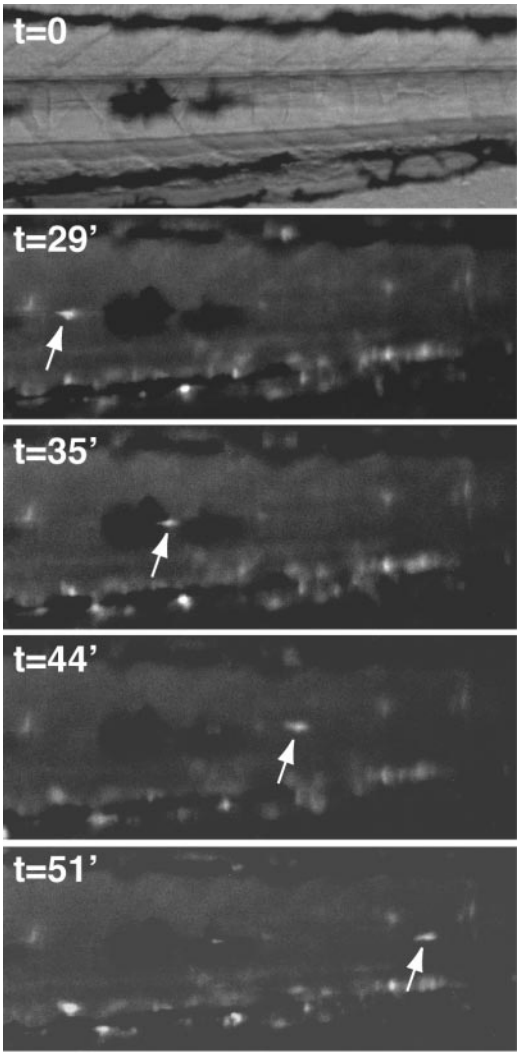

Fig. 4. Migration of a zMPO:GFP leukocyte through embryonic tissues. Images from a time-lapse movie of the midbody of a zMPO:GFP embryo at 3 dpf. At the top is an oblique coherent contrast image corresponding to the first frame of the movie; below are fluorescence images captured at the times indicated. The arrow indicates a single GFP+ cell that migrates across the midbody, apparently outside of the vasculature, over an ~20-min period.

was 9.94 ± 0.36 μm/min, which is comparable with the in vitro motility observed for human neutrophils [19]. A slower-moving (3.50 ± 0.50 μm/min) cell type, which faintly expresses GFP, was also observed to migrate toward wound sites (Fig. 5, arrowheads). These cells exhibited an elongated morphology distinct from neutrophils and usually arrived at a wound site after the first-arriving neutrophils. Based on these characteristics and previous observations [21], we anticipate that these cells may represent a subpopulation of the monocyte/macrophage lineage [22], which has been shown to exhibit a low level of MPO activity [23].

Zebrafish neutrophils demonstrate retrograde chemotaxis toward the vasculature

To address the resolution phase of the inflammatory response, neutrophil trafficking was observed for extended times after wounding. It is interesting that zebrafish neutrophils displayed retrograde chemotaxis from the wound site back toward the vasculature (Figs. 5, bottom, and 6, B–D), implicating retrograde migration as a mechanism involved in resolving the inflammatory response. We observed no apparent apoptosis of neutrophils at wound sites during the course of any time-lapse movie, even in those with a significant (up to ~10 cells) and prolonged inflammatory response (data not shown). Rather, the majority of cells that entered the wound (more than 80%) was observed to track back toward the vasculature, the remainder of which were usually still migrating around wound sites at the end of individual movies. To quantify the migration and to determine the significance of the retrograde chemotaxis, migration velocity and directionality were calculated from tracks of neutrophils migrating toward (**Fig. 7A**) or away from (Fig. 7B) fin wounds. Directionality can be calculated by determining the ratio of the shortest linear distance traveled compared with the total distance traveled (D/T), as described in Materials and Methods. It is interesting that the velocity and directionality were comparable for neutrophils traveling toward the wound and back toward the vasculature (Fig. 7C). Furthermore, the majority of directionality measurements indicated that the migration tracks were highly directional (average D/T=0.7) and not the result of random motility. These observations indicate that the retrograde chemotaxis back toward the vasculature is an active process, comparable with the motility response directed toward the wound.

Further analysis of neutrophil motility in response to wounding indicated that different neutrophils were observed to display simultaneous, bidirectional migration (Supplemental Movie 3). This suggests that after stopping at a wound, individual neutrophils gain the ability to respond to signals other than those generated from the wound site, rather than having a global cessation of the wound signal that limits neutrophil recruitment at a specific time. Together, our findings suggest that retrograde migration away from wound sites may constitute a mechanism by which neutrophilic inflammation is resolved.

DISCUSSION

We have generated a novel transgenic zebrafish in which neutrophil chemotaxis and inflammatory responses can be visualized with high resolution in vivo. This system provides a genetically tractable model of zebrafish inflammatory responses and also represents a powerful tool to dissect mechanisms that modulate neutrophil polarization and chemotaxis in vivo. Using this model, we have identified a unique mechanism of neutrophil trafficking between sites of tissue injury and the vasculature.

The mechanisms that resolve inflammation have remained elusive because of the limited tools available to image inflammation in vivo. Recent reviews [11, 13] have indicated that neutrophil-mediated inflammation is resolved by regulated apoptosis of neutrophils in inflamed tissue. In contrast, our findings indicate that neutrophils traffick bidirectionally between sites of tissue injury and the vasculature, suggesting that retrograde neutrophil chemotaxis to the vasculature may provide a novel and important mechanism by which inflammation is resolved. It is interesting that our findings demonstrate that

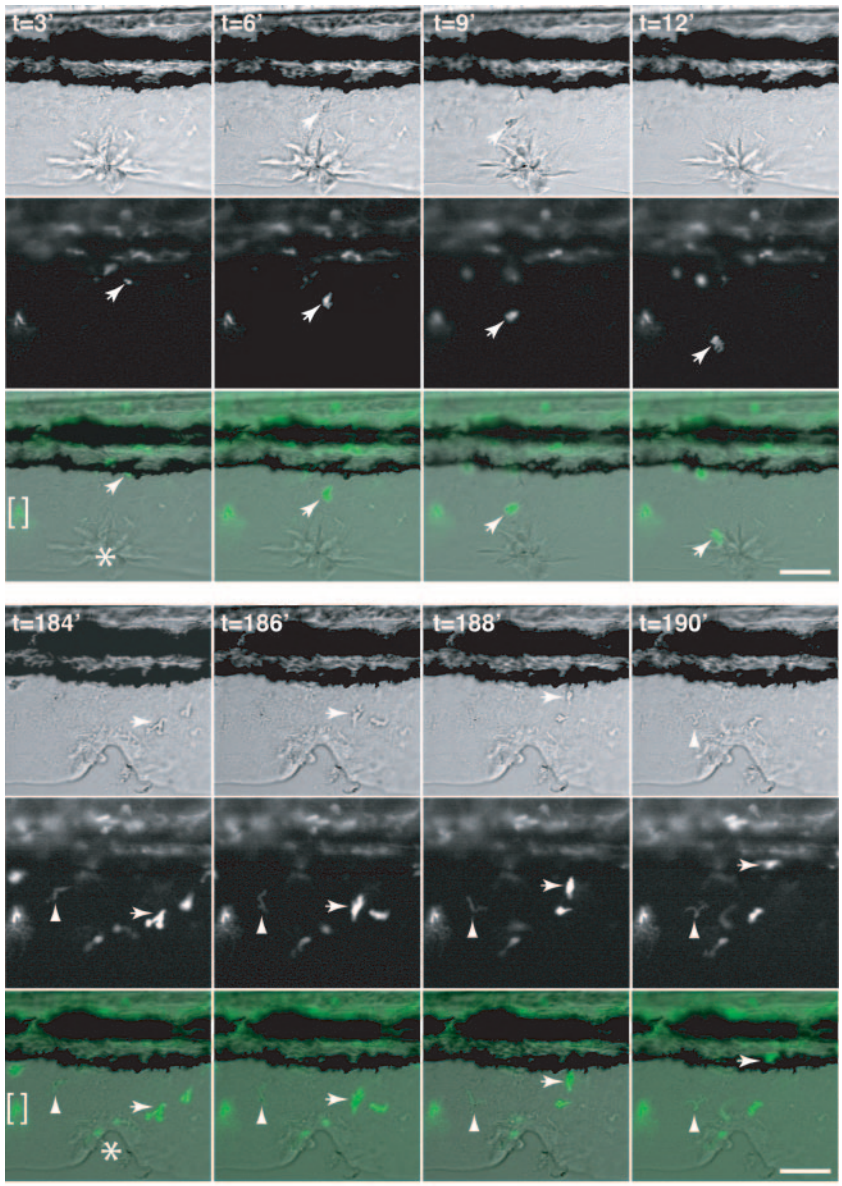

Fig. 5. Time-lapse microscopy of zMPO:GFP leukocyte migration in response to a wound. A zMPO:GFP embryo at 3 dpf was wounded (denoted by *) in the ventral fin (just below the ICM) and maintained in media containing Tricaine. Two sequences from the same movie (Supplemental Movie 3) are shown, and each set consists of three rows: DIC (top row), green fluorescence (middle row), and overlay (bottom row). The top sequence consists of 3-min intervals, starting at 3 min after wounding (other times also indicate post-wound) and depicts a single neutrophil (marked by an arrow in each frame) migrating toward the wound. The bottom sequence consists of 2-min intervals starting 184 min post-wound. In this series, a neutrophil (marked by an arrow) migrates away from the wound, and a dim GFP+ cell (marked by an arrowhead) moves toward the wound. For each sequence, the position of each marked cell is indicated in the DIC images when possible. In the left-most panel of each overlay series, a nonmigrating, GFP-expressing fin cell is indicated in brackets. Also note (in DIC images) the shedding of wounded fin cells that occurs in between the two sequences, which are 3 h apart. Original bars represent 50 μm.

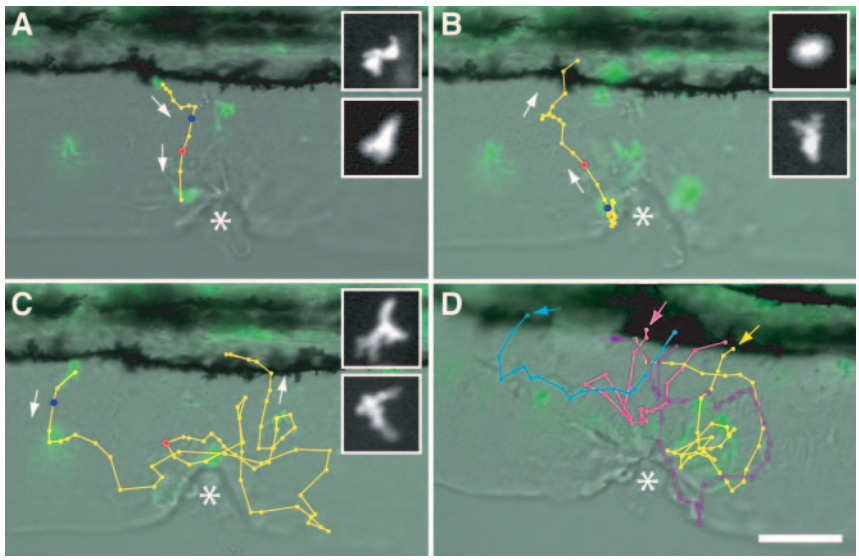

Fig. 6. Tracking and morphology of migrating zMPO:GFP neutrophils. (A–C) Individual neutrophils in Supplemental Movie 3 were tracked using MetaMorph software as described in Materials and Methods. Each individual cell track is overlaid onto the first frame of the track to indicate the starting position of the cell. Closed circles indicate the position of the cell for each frame (1 min between each frame), and arrows indicate the direction of migration. For each panel, fluorescence images (inset boxes, 30 μm per side) are shown for two time-points to display cellular morphology; each upper inset shows the time-point indicated by a blue dot on the track, and the lower inset is indicated by a red dot. (A) Track from Frames 32–43; a neutrophil migrating from the vasculature to the wound. (B) Frames 71–100; a neutrophil migrating from the wound to the vasculature/ICM. (C) Frames 130–193; a neutrophil migrating from the vasculature to the wound and then around the wound and back to the vasculature/ICM. (D) Four separate cell tracks (taken from a different movie) from the vasculature to the wound and back to the vasculature; arrows indicate the start of each individual track. Bar represents 50 μm; *, wound.

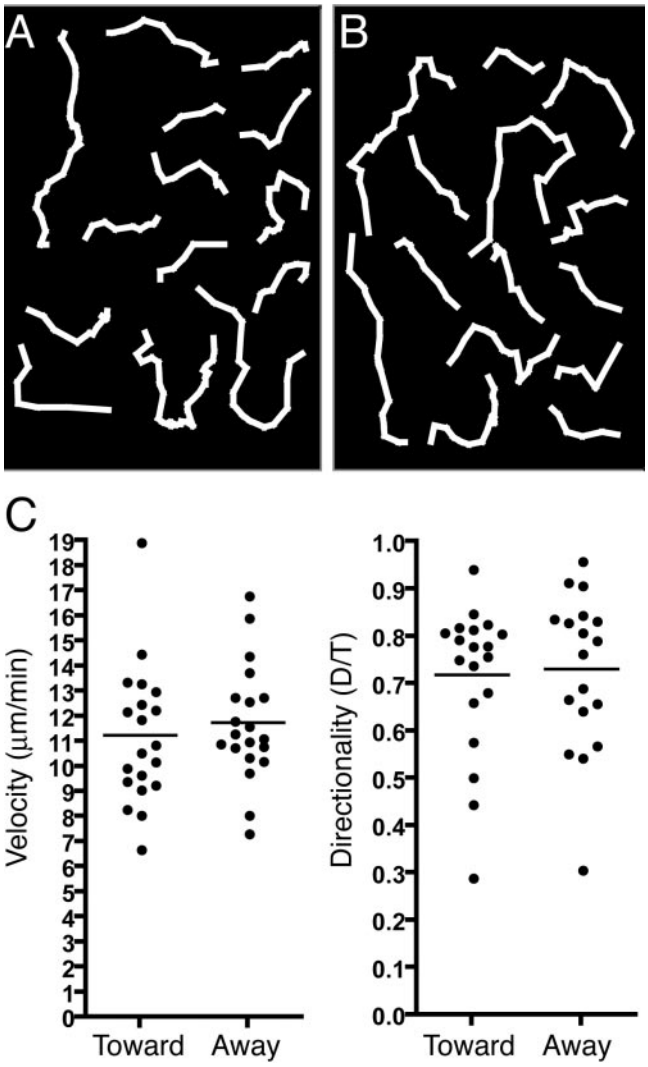

Fig. 7. Neutrophil migration velocity and directionality. (A and B) Representative examples of cell tracks taken by neutrophils migrating toward the wound (A) or toward the vasculature (B). The data represent tracks from multiple experiments and are not oriented with respect to the wound or vasculature. (C) Graphs of cell velocity and directionality (D/T) for individual neutrophils (●) migrating toward ($n=20$) or away from ($n=20$) the wound. Note that these data were calculated only from tracks of cells that were actively migrating toward or away from the wound. Bars indicate average velocity or directionality.

leukocyte velocity and directionality are the same to and from the wound, indicating that the retrograde chemotaxis is an active process and is not the result of random motility. There has been speculation of this "round-trip" migration by neutrophils and other leukocytes [24], and we now provide direct evidence to support this model. Our findings are in accordance with a recent report that indicates that neutrophils can undergo retrograde migration across the endothelium after transendothelial migration [25]. Taken together, these studies and our observations suggest that retrograde chemotaxis may complement regulated neutrophil apoptosis to resolve inflammation. To study this possibility further, we are developing zebrafish models of chronic inflammation induced by genetic mutations (J. R. Mathias, unpublished observations) or bacterial infections as previously reported [26, 27].

A challenge for future investigation will be to determine the factors that modulate bidirectional motility and to further dissect how a neutrophil prioritizes these competing signals in vivo. It is interesting that we detected simultaneous, bidirectional trafficking between the wound and vasculature, suggesting that neutrophils are able to migrate back to the vasculature in the presence of active, migration-inducing signals at the wound. Although we are not certain of the signals that regulate this process, it appears that neutrophils responding to a wound are prioritizing opposing signals from the wound and the vasculature. Recent studies have shown that chemoattractant signals can also induce retrograde chemotaxis ("fugetaxis") away from high concentrations of the signal [28]. It is possible that conditions may be present in the immediate vicinity of a wound site, which induces fugetaxis. Chemokine communication from other later-arriving blood cells may also induce retrograde movement of neutrophils, which have been shown to interact with other blood cells through secreted signals [29] and cell-to-cell contacts [30].

Our findings suggest that mutations or exogenous agents that affect neutrophil chemotaxis may lead to neutrophil retention and chronic inflammation. Accordingly, we recently reported that a patient with the chronic inflammatory disease, neonatal onset multisystem inflammatory disease, and a mutation in cryopyrin displayed reduced neutrophil chemotaxis in vitro [31]. It is possible that this reduced capacity for chemotaxis may have contributed to chronic neutrophilic inflammation by reducing the resolution phase by retrograde chemotaxis. Our findings also demonstrate that zebrafish neutrophils often arrest at wound sites prior to trafficking back to the vasculature (Fig. 6B), exhibiting a rounded morphology and loss of pseudopod extension similar to observations of arrested lymphocytes in vivo [32]. This suggests that loss of "stop" signals may be a key switch involved in resolving inflammation and that if improperly regulated, may result in the retention of neutrophils within an inflamed area. In recent in vitro studies, we provide evidence that TNF-α may provide such a stop signal to human neutrophils and reduce sensitivity to other chemotactic stimuli [33].

In addition to providing key insight into how neutrophils traffick and contribute to inflammation, this transgenic zebrafish provides a novel tool to identify the mechanism of action of anti-inflammatory agents and is amenable to high-throughput screening of small molecule compounds that may aid in the identification of novel therapeutic agents [1]. A recent study accentuates the potential of this system, as chemotaxis of embryonic zebrafish macrophages was disrupted by treatment with the microtubule-destabilizing drug nocodazole [34]. In addition, the random motility of zebrafish neutrophils through bodily tissues (Fig. 4 and Supplemental Movie 2), which we observed, can potentially be used as an indicator of neutrophil viability in response to drug treatments or to specifically identify agents that affect neutrophil chemotaxis without affecting random motility in vivo.

In summary, we have developed a novel technology that will provide a powerful tool for understanding inflammation in vivo and can be used for genetic or chemical screens. The identification of signaling pathways that modulate these specific

stages of the inflammatory response may provide key insight into novel therapeutic targets that may be used to limit the inflammatory response. The further analysis of neutrophil trafficking in the context of chronic inflammatory zebrafish models will also provide important insight into how these mechanisms may go awry and contribute to chronic inflammation.

ACKNOWLEDGMENTS

This work was supported by National Institutes of Health (NIH) Grants R01 GM074827 (A. H.) and CA-93152 (A. T. L.), University of Wisconsin Hematology Training Grant T32 HL07899-07 (J. R. M.), and Arthritis Foundation Postdoctoral Fellowship (J. R. M.). The Zebrafish International Resource Center is supported by Grant P40 RR12546 from the NIH-National Center for Research Resources. We gratefully acknowledge Jennifer Rhodes (for extensive help with the manuscript), Mary Lokuta (for help with cell tracking), Kate Cooper (for construction of the GST-zMPO plasmid and zebrafish maintenance), David Bennin (for purification of GST-zMPO protein and zMPO antibody production), Vikrum Vishnubhakta (for zMPO antibody production), M. Ernest Dodd (for critical reading of the manuscript and zebrafish maintenance), Vanessa Ott (for critical reading of the manuscript), and Brian Kayon, Fred Kohlhapp, Christa Cortesio, and Ellen Thompson (for zebrafish maintenance).

REFERENCES

1. Zon, L. I., Peterson, R. T. (2005) In vivo drug discovery in the zebrafish. *Nat. Rev. Drug Discov.* **4,** 35–44.
2. Amsterdam, A., Burgess, S., Golling, G., Chen, W., Sun, Z., Townsend, K., Farrington, S., Haldi, M., Hopkins, N. (1999) A large-scale insertional mutagenesis screen in zebrafish. *Genes Dev.* **13,** 2713–2724.
3. Patton, E. E., Zon, L. I. (2001) The art and design of genetic screens: zebrafish. *Nat. Rev. Genet.* **2,** 956–966.
4. Trede, N. S., Langenau, D. M., Traver, D., Look, A. T., Zon, L. I. (2004) The use of zebrafish to understand immunity. *Immunity* **20,** 367–379.
5. De Jong, J. L., Zon, L. I. (2005) Use of the zebrafish system to study primitive and definitive hematopoiesis. *Annu. Rev. Genet.* **39,** 481–501.
6. Crowhurst, M. O., Layton, J. E., Lieschke, G. J. (2002) Developmental biology of zebrafish myeloid cells. *Int. J. Dev. Biol.* **46,** 483–492.
7. Onnebo, S. M., Yoong, S. H., Ward, A. C. (2004) Harnessing zebrafish for the study of white blood cell development and its perturbation. *Exp. Hematol.* **32,** 789–796.
8. Lieschke, G. J., Oates, A. C., Crowhurst, M. O., Ward, A. C., Layton, J. E. (2001) Morphologic and functional characterization of granulocytes and macrophages in embryonic and adult zebrafish. *Blood* **98,** 3087–3096.
9. Bennett, C. M., Kanki, J. P., Rhodes, J., Liu, T. X., Paw, B. H., Kieran, M. W., Langenau, D. M., Delahaye-Brown, A., Zon, L. I., Fleming, M. D., Look, A. T. (2001) Myelopoiesis in the zebrafish, *Danio rerio*. *Blood* **98,** 643–651.
10. Henson, P. M. (2005) Dampening inflammation. *Nat. Immunol.* **6,** 1179–1181.
11. Serhan, C. N., Savill, J. (2005) Resolution of inflammation: the beginning programs the end. *Nat. Immunol.* **6,** 1191–1197.
12. Haslett, C. (1999) Granulocyte apoptosis and its role in the resolution and control of lung inflammation. *Am. J. Respir. Crit. Care Med.* **160,** S5–11.
13. Dockrell, D. H., Whyte, M. K. (2006) Regulation of phagocyte lifespan in the lung during bacterial infection. *J. Leukoc. Biol.* **79,** 904–908.
14. Nusslein-Volhard, C., Dahm, R. (2002) *Zebrafish, A Practical Approach*, New York, NY, Oxford University Press.
15. Kimmel, C. B., Ballard, W. W., Kimmel, S. R., Ullmann, B., Schilling, T. F. (1995) Stages of embryonic development of the zebrafish. *Dev. Dyn.* **203,** 253–310.
16. Bennin, D. A., Don, A. S., Brake, T., McKenzie, J. L., Rosenbaum, H., Ortiz, L., DePaoli-Roach, A. A., Horne, M. C. (2002) Cyclin G2 associates with protein phosphatase 2A catalytic and regulatory B' subunits in active complexes and induces nuclear aberrations and a G1/S phase cell cycle arrest. *J. Biol. Chem.* **277,** 27449–27467.
17. Traver, D., Paw, B. H., Poss, K. D., Penberthy, W. T., Lin, S., Zon, L. I. (2003) Transplantation and in vivo imaging of multilineage engraftment in zebrafish bloodless mutants. *Nat. Immunol.* **4,** 1238–1246.
18. Lin, H. F., Traver, D., Zhu, H., Dooley, K., Paw, B. H., Zon, L. I., Handin, R. I. (2005) Analysis of thrombocyte development in CD41-GFP transgenic zebrafish. *Blood* **106,** 3803–3810.
19. Lokuta, M. A., Nuzzi, P. A., Huttenlocher, A. (2003) Calpain regulates neutrophil chemotaxis. *Proc. Natl. Acad. Sci. USA* **100,** 4006–4011.
20. Pankov, R., Endo, Y., Even-Ram, S., Araki, M., Clark, K., Cukierman, E., Matsumoto, K., Yamada, K. M. (2005) A Rac switch regulates random versus directionally persistent cell migration. *J. Cell Biol.* **170,** 793–802.
21. Herbomel, P., Thisse, B., Thisse, C. (2001) Zebrafish early macrophages colonize cephalic mesenchyme and developing brain, retina, and epidermis through a M-CSF receptor-dependent invasive process. *Dev. Biol.* **238,** 274–288.
22. Gordon, S., Taylor, P. R. (2005) Monocyte and macrophage heterogeneity. *Nat. Rev. Immunol.* **5,** 953–964.
23. Kaplow, L. S. (1965) Simplified myeloperoxidase stain using benzidine dihydrochloride. *Blood* **26,** 215–219.
24. Badolato, R. (2004) Leukocyte circulation: one-way or round-trip? Lessons from primary immunodeficiency patients. *J. Leukoc. Biol.* **76,** 1–6.
25. Buckley, C. D., Ross, E. A., McGettrick, H. M., Osborne, C. E., Haworth, O., Schmutz, C., Stone, P. C., Salmon, M., Matharu, N. M., Vohra, R. K., Nash, G. B., Rainger, G. E. (2006) Identification of a phenotypically and functionally distinct population of long-lived neutrophils in a model of reverse endothelial migration. *J. Leukoc. Biol.* **79,** 303–311.
26. Davis, J. M., Clay, H., Lewis, J. L., Ghori, N., Herbomel, P., Ramakrishnan, L. (2002) Real-time visualization of mycobacterium-macrophage interactions leading to initiation of granuloma formation in zebrafish embryos. *Immunity* **17,** 693–702.
27. van der Sar, A. M., Musters, R. J., van Eeden, F. J., Appelmelk, B. J., Vandenbroucke-Grauls, C. M., Bitter, W. (2003) Zebrafish embryos as a model host for the real time analysis of *Salmonella typhimurium* infections. *Cell. Microbiol.* **5,** 601–611.
28. Tharp, W. G., Yadav, R., Irimia, D., Upadhyaya, A., Samadani, A., Hurtado, O., Liu, S. Y., Munisamy, S., Brainard, D. M., Mahon, M. J., Nourshargh, S., van Oudenaarden, A., Toner, M. G., Poznansky, M. C. (2006) Neutrophil chemorepulsion in defined interleukin-8 gradients in vitro and in vivo. *J. Leukoc. Biol.* **79,** 539–554.
29. Nathan, C. (2006) Neutrophils and immunity: challenges and opportunities. *Nat. Rev. Immunol.* **6,** 173–182.
30. Megiovanni, A. M., Sanchez, F., Robledo-Sarmiento, M., Morel, C., Gluckman, J. C., Boudaly, S. (2006) Polymorphonuclear neutrophils deliver activation signals and antigenic molecules to dendritic cells: a new link between leukocytes upstream of T lymphocytes. *J. Leukoc. Biol.* **79,** 977–988.
31. Lokuta, M. A., Cooper, K. M., Aksentijevich, I., Kastner, D. L., Huttenlocher, A. (2005) Neutrophil chemotaxis in a patient with neonatal-onset multisystem inflammatory disease and Muckle-Wells syndrome. *Ann. Allergy Asthma Immunol.* **95,** 394–399.
32. Bhakta, N. R., Oh, D. Y., Lewis, R. S. (2005) Calcium oscillations regulate thymocyte motility during positive selection in the three-dimensional thymic environment. *Nat. Immunol.* **6,** 143–151.
33. Lokuta, M. A., Huttenlocher, A. (2005) TNF-{α} promotes a stop signal that inhibits neutrophil polarization and migration via a p38 MAPK pathway. *J. Leukoc. Biol.* **78,** 210–219.
34. Redd, M. J., Kelly, G., Dunn, G., Way, M., Martin, P. (2006) Imaging macrophage chemotaxis in vivo: studies of microtubule function in zebrafish wound inflammation. *Cell Motil. Cytoskeleton* **63,** 415–422.